minimum interval of 905 ms (55 frames). The experiment consisted of 12 blocks of 40 trials each, resulting in 120 trials per experimental condition. Blocks were administered in random order. The responding hand was changed halfway through the experiment, and the sequence of hand usage was counterbalanced across subjects. One subject was excluded from further analysis because of difficulty in detecting the matching symbols.

Data acquisition

The electrode positions shown schematically in Fig. 1 are specified in a previous report[30]. The EEG was recorded with a sampling rate of 250 Hz and a bandpass of d.c. to 50 Hz. Individual trials were discarded on the basis of blink or electromyogram (EMG) artefacts in the scalp channels exceeding 75 μV, or when lateral eye movements monitored in the horizontal electro-oculogram (EOG) deviated more than 11 μV (1°) from fixation. These stringent criteria resulted in a mean rejection rate of 30% of the trials. In order to analyse the SSVEP, artefact-free EEG epochs were averaged separately for each experimental condition and algebraically re-referenced to averaged mastoids by subtracting one-half of the averaged signal recorded from the mastoid opposite the reference mastoid from the averaged signals at each scalp site. The averaging epochs extended from 500 ms before to 2,500 ms after the time point when all streams were synchronized (that is, from 26 to 3,026 ms after flicker onset). SSVEP amplitudes were extracted by means of complex demodulation of the averaged waveforms[15,19,25]. To avoid including the visual evoked response to flicker onset in the SSVEP measurements, the first 500 ms of each epoch were excluded from analysis. Thus, mean SSVEP amplitudes were calculated over the interval 526 to 3,026 ms after flicker onset.

Data analysis

For testing the significance of SSVEP amplitude changes, the posterior electrode site that exhibited the largest overall attention effect (comparing attended versus ignored positions) was selected for each subject. These amplitude values were subjected to paired *t*-tests between conditions, and corrected for multiple comparisons by the Bonferroni–Dunn criterion. As a reliability check, the averaged amplitudes across three standard electrode locations (PO3/4, PO7/8 and O1/2) were also subjected to paired *t*-tests for the attended versus ignored SSVEPs at 8.69 Hz and 20.27 Hz under conditions of attention to separated locations.

Only button-presses occurring between 250 and 1,000 ms after target-pair onset were accepted as correct detections. False alarms for the adjacent condition were defined as button presses occurring in response to a target presented at only one of the attended locations. For the separate conditions, false alarms were defined as button presses in response to a target presented in only one of the attended locations and/or in the intermediate to-be-ignored position. Target detection rates, reaction times and false alarms were tested by one factor repeated measures analysis of variance (experimental condition).

Received 3 April; accepted 27 May 2003; doi:10.1038/nature01812.

1. LaBerge, D. *Attentional Processing* (Harvard Univ. Press, Cambridge, Massachusetts, 1995).
2. Posner, I. P. & Petersen, S. E. The attention system of the human brain. *Annu. Rev. Neurosci.* **13,** 25–42 (1990).
3. Eriksen, C. W. & Yeh, Y. Y. Allocation of attention in the visual field. *J. Exp. Psychol. Hum. Percept. Perform.* **11,** 583–597 (1985).
4. LaBerge, D. & Brown, V. Theory of attentional operations in shape identification. *Psychol. Rev.* **96,** 101–124 (1989).
5. Shaw, M. L. & Shaw, P. Optimal allocation of cognitive resources to spatial locations. *J. Exp. Psychol. Hum. Percept. Perform.* **3,** 201–211 (1977).
6. Castiello, U. & Umilta, C. Splitting focal attention. *J. Exp. Psychol. Hum. Percept. Perform.* **18,** 837–848 (1992).
7. Posner, M. I., Snyder, C. R. R. & Davidson, B. J. Attention and detection of signals. *J. Exp. Psychol. Gen.* **109,** 160–174 (1980).
8. Pan, K. & Eriksen, C. W. Attentional distribution in the visual field during same-different judgements as assessed by response competition. *Percept. Psychophys.* **53,** 134–144 (1993).
9. McCormick, P. A., Klein, R. M. & Johnston, S. Splitting vs. shared visual attention: An empirical commentary on Castiello & Umilta (1992). *J. Exp. Psychol. Hum. Percept. Perform.* **24,** 350–357 (1998).
10. Kiefer, R. J. & Siple, P. Spatial constraints on the voluntary control of attention across visual space. *Can. J. Psychol.* **41,** 474–489 (1987).
11. Eimer, M. Attending to quadrants and ring-shaped regions: ERP effects of visual attention in different spatial selection tasks. *Psychophysiology* **36,** 491–503 (1999).
12. Heinze, H.-J. *et al.* Attention to adjacent and separate positions in space: An electrophysiological analysis. *Percept. Psychophys.* **56,** 42–52 (1994).
13. Awh, E. & Pashler, H. Evidence for split attentional foci. *J. Exp. Psychol. Hum. Percept. Perform.* **26,** 834–846 (2000).
14. Hahn, S. & Kramer, A. F. Further evidence for the division of attention between noncontiguous locations. *Vis. Cognit.* **5,** 217–256 (1998).
15. Regan, D. *Human Brain Electrophysiology: Evoked Potentials and Evoked Magnetic Fields in Science and Medicine* (Elsevier, New York, 1989).
16. Müller, M. M. *et al.* Effects of spatial selective attention on the steady-state visual evoked potential in the 20–28 Hz range. *Cognit. Brain Res.* **6,** 249–261 (1998).
17. Di Russo, F. & Spinelli, D. Spatial attention has different effects on the magno- and parvocellular pathways. *NeuroReport* **10,** 2755–2762 (1999).
18. Müller, M. M., Teder-Sälejärvi, W. & Hillyard, S. A. The time course of cortical facilitation during cued shifts of spatial attention. *Nature Neurosci.* **1,** 631–634 (1998).
19. Müller, M. M. *et al.* in *Oscillatory Event-related Brain Dynamics* (eds Pantev, C., Elbert, T. & Lütkenhöner, B.) 325–342 (Plenum, New York, 1994).
20. Reeves, A. & Sperling, G. Attention gating in short-term visual memory. *Psychol. Rev.* **93,** 180–206 (1986).
21. Weichselgartner, E. & Sperling, G. Dynamics of automatic controlled visual attention. *Science* **238,** 778–780 (1987).
22. Duncan, J., Ward, R. & Shapiro, K. Direct measurement of attentional dwell time in human vision. *Nature* **369,** 313–315 (1994).
23. Peterson, M. S. & Juola, J. F. Evidence for distinct attentional bottlenecks in attention switching and attentional blink tasks. *J. Gen. Psychol.* **127,** 6–26 (2000).
24. Moore, C. M., Egeth, H., Berglan, L. & Luck, S. J. Are attentional dwell times inconsistent with serial visual search? *Psychonom. Bull. Rev.* **3,** 360–365 (1996).
25. Müller, M. M. & Hübner, R. Can the attentional spotlight be shaped like a doughnut? Evidence from steady state visual evoked potentials. *Psychol. Sci.* **13,** 119–124 (2002).
26. Müller, M. M., Teder, W. & Hillyard, S. A. Magentoencephalographic recording of steady-state visual evoked cortical activity. *Brain Topogr.* **9,** 163–168 (1997).
27. Hillyard, S. A. *et al.* Combining steady-state visual evoked potentials and fMRI to localize brain activity during selective attention. *Hum. Brain Mapp.* **5,** 287–292 (1997).
28. Clark, V. P. & Hillyard, S. A. Spatial selective attention affects early extrastriate but not striate components of the visual evoked potential. *J. Cognit. Neurosci.* **8,** 387–402 (1996).
29. Martinez, A. *et al.* Putting spatial attention on the map: Timing and localization of stimulus selection processes in striate and extrastriate visual areas. *Vis. Res.* **41,** 1437–1457 (2001).
30. Clark, V. P., Fan, S. & Hillyard, S. A. Identification of early visual evoked potential generators by retinotopic and topographic analyses. *Hum. Brain Mapp.* **2,** 170–187 (1995).

Acknowledgements We thank N. Williams, H. Messmer and C.-M. Giabbiconi for help in data recording. This work was supported by the Deutsche Forschungsgemeinschaft and by NIMH.

Competing interests statement The authors declare that they have no competing financial interests.

Correspondence and requests for materials should be addressed to M.M.M. (m.mueller@rz.uni-leipzig.de).

Perceptual consequences of centre–surround antagonism in visual motion processing

Duje Tadin, Joseph S. Lappin, Lee A. Gilroy & Randolph Blake

Vanderbilt Vision Research Center, Vanderbilt University, 111 21st Avenue South, Nashville, Tennessee 37203, USA

Centre–surround receptive field organization is a ubiquitous property in mammalian visual systems, presumably tailored for extracting image features that are differentially distributed over space[1]. In visual motion, this is evident as antagonistic interactions between centre and surround regions of the receptive fields of many direction-selective neurons in visual cortex[2–6]. In a series of psychophysical experiments we make the counterintuitive observation that increasing the size of a high-contrast moving pattern renders its direction of motion more difficult to perceive and reduces its effectiveness as an adaptation stimulus. We propose that this is a perceptual correlate of centre–surround antagonism, possibly within a population of neurons in the middle temporal visual area. The spatial antagonism of motion signals observed at high contrast gives way to spatial summation as contrast decreases. Evidently, integration of motion signals over space depends crucially on the visibility of those signals, thereby allowing the visual system to register motion information efficiently and adaptively.

Centre–surround neurons, especially those in the middle temporal visual area (MT), are believed to be crucially involved in the perception of object motion[3,7], in figure–ground segmentation[7–9] and in the registration of three-dimensional shape from motion[9,10]. By analogy with other aspects of vision[11], if centre–surround antagonism is an integral part of motion processing, we should expect to see a perceptual signature of this antagonism in the form of impaired motion visibility with increasing stimulus size. However, existing evidence shows that increasing the size of a low-contrast moving stimulus enhances its visibility[12,13], presumably

owing to spatial summation. Such psychophysical estimations of the spatial properties of motion mechanisms tend to be based on low-contrast or noisy stimuli, whereas physiological descriptions of centre–surround motion neurons have been obtained with high-contrast motion. Moreover, in the visual cortex, the nature of centre–surround interactions is often dependent on contrast: surround suppression is stronger at high contrast and spatial summation is more pronounced at low contrast[14–16]. Thus, threshold contrast measurements might not fully describe the spatial properties of human motion perception, especially at high contrast. With this in mind, we devised alternative approaches for measuring motion sensitivity.

In our first experiment we measured the threshold exposure duration required for human observers to accurately identify the motion direction of a drifting Gabor patch. In separate conditions, observers viewed foveally presented Gabor patches of various sizes and contrasts. Spatial frequency and speed were fixed at 1 cycle per degree and $2^\circ\,s^{-1}$, respectively. The contrast of a Gabor patch was ramped on and off with a temporal gaussian envelope, allowing the presentation of brief motion stimuli.

Increasing stimulus contrast resulted in a marked change in the way in which motion signals were integrated over space (Fig. 1). At low contrast (2.8%), duration thresholds decreased with increasing size, reaching a lower asymptote at about 40 ms (Fig. 1a, c). This result, implying spatial summation of motion signals, is consistent with earlier reports[12,13]. At high contrast, however, duration thresholds increased fourfold as the Gabor patch width increased from 0.7° to 5°. In other words, for small Gabor patches, performance improved with increasing contrast, whereas for large Gabor patches, performance deteriorated substantially with contrast (Fig. 1b). These highly surprising results imply neural processes fundamentally different from spatial summation. Closer examination of the results reveals that the increase in duration threshold was greatest for Gabor patches larger than 2.7° in width (arrow in Fig. 1b), indicating the existence of a 'critical size'. We speculated that surround inhibition might be responsible for the observed decrease in motion sensitivity, leading us to explore this hypothesis in several more experiments.

Similar contrast-dependent size effects were obtained with faster-moving stimuli ($8^\circ\,s^{-1}$) and with Gabor patches whose spatial bandwidth was held constant by scaling spatial frequency (1 cycle per σ). We also manipulated the effective stimulus contrast by adding variable amounts of dynamic noise to a fixed-contrast Gabor patch. We found evidence for spatial summation when motion appeared within high-contrast noise, and evidence for spatial suppression when motion appeared within weak noise or when noise was absent altogether (Fig. 2a). In other words, the presence of noise actually improved the visibility of large-motion stimuli.

Most neurophysiological explorations of centre–surround motion neurons have been performed with spatially broadband random-dot displays. We therefore also investigated effects of size with random-dot stimuli (light and dark pixels, each 3 × 3 arcmin) presented in a spatial gaussian envelope. From frame to frame of the animation, half of the pixels shifted in one direction ($6.2^\circ\,s^{-1}$) while the remaining pixels were randomly regenerated, conditions producing vivid motion perception at suprathreshold exposure durations. Duration thresholds with these stimuli, too, yielded evidence for spatial summation at low contrast and spatial suppression at high contrast (Fig. 2b).

Realizing that the receptive field sizes of motion-sensitive neurons increase with retinal eccentricity[6,17], we wondered whether the detrimental effect of stimulus size at high contrast would diminish with increasing eccentricity. Accordingly, we manipulated the display size for a range of eccentricities with contrast fixed at 92%. Once again, foveal presentation yielded evidence for surround suppression (Fig. 2c). As eccentricity increased, duration thresholds decreased for all sizes. More importantly, the size dependence of duration thresholds changed systematically with eccentricity, with almost no effect at the largest eccentricity tested.

The motion strength of a periodic Gabor patch can also be varied

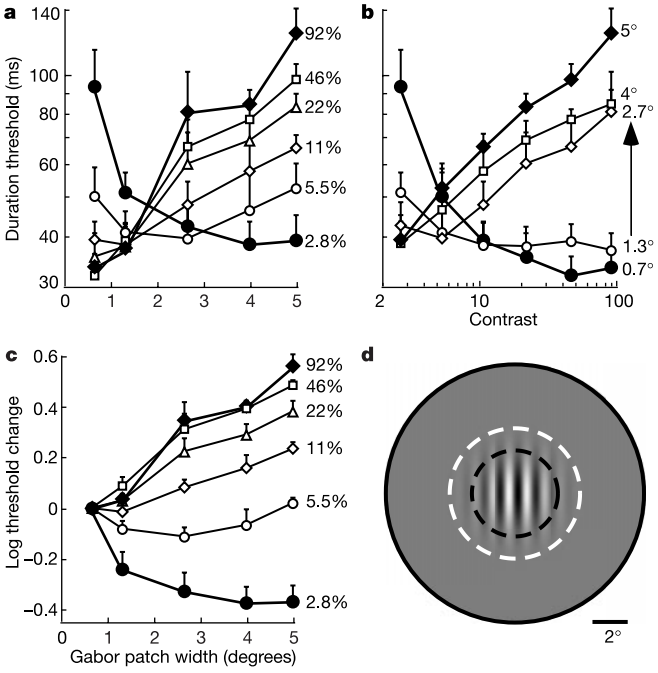

Figure 1 Effects of size and contrast on motion perception. Individual data points are averages for five observers. Results are means ± s.e.m. **a**, Duration thresholds as a function of stimulus size at different contrasts. **b**, Duration thresholds as a function of contrast for a range of stimulus sizes. **c**, Log of threshold change as a function of stimulus size at different contrasts. For each observer, the logarithm of the threshold change was calculated relative to the duration threshold for the smallest size (0.7°) at each contrast level. Note that the transition from suppression to summation occurs at about 5% contrast, a value that, coincidentally or not, is the contrast in which MT neurons attain about 25% of their maximum response on average[28]. **d**, A Gabor patch 2.7° wide shown relative to an average foveal macaque MT receptive field. The dashed dark circle illustrates the stimulus size beyond which an average foveal MT centre–surround neuron exhibits surround suppression[6]. The radius of the surround is usually about three times the centre radius, as indicated by the full circle. The full spatial extent of the Gabor patch ($r = 3\sigma = 4°$) is indicated by the white dashed circle. This comparison assumes that the properties of human and macaque MT are comparable[29] and that the receptive field sizes are similar for the two species[30].

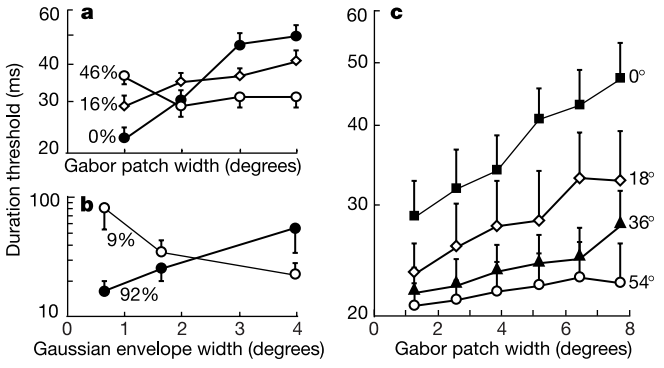

Figure 2 Results from added-noise, random-dot and eccentricity experiments. **a**, Duration thresholds as a function of stimulus size at different noise contrasts. **b**, Duration thresholds as a function of random-dot stimulus size at different contrasts. **c**, Duration thresholds as a function of stimulus size at different eccentricities. Results are means ± s.e.m.

by adjusting the magnitude of an abrupt phase shift[18]: increasing phase shifts from 0° to 90° enhances the visibility of motion. We conducted an experiment in which observers identified the motion direction of a fixed-contrast Gabor patch that abruptly shifted in phase in the middle of a 100-ms presentation interval. Threshold phase shift was obtained for a range of contrasts and sizes with spatial frequency fixed at 0.5 cycle per degree. Results (Fig. 3a) replicated the duration threshold findings, again showing the spatial suppression of motion signals at high contrast.

Given the reduced visibility of isoluminant moving stimuli[19], we might expect spatial summation of isoluminant stimuli similar to that observed for low-contrast and noisy stimuli. Using the phase-shift procedure from the previous experiment, we compared thresholds for isoluminant (red–green) and high-luminance contrast (yellow–black) Gabor patches. Once again, luminance contrast stimuli exhibited surround suppression (Fig. 3b). However, thresholds for isoluminant stimuli decreased with increasing size, exhibiting spatial summation. This result is surprising in that colour-defined motion with large stimuli was actually perceived more accurately than luminance-defined motion, presumably because the latter is affected by surround suppression.

Surround inhibition in motion-sensitive neurons decreases neural activity in response to a large moving stimulus. This decreased activity might be evident in weaker adaptation of motion-sensitive centre–surround neurons during prolonged exposure to motion. The motion after-effect (MAE)—an illusory perception of motion after prolonged exposure to motion—is thought to reflect the adaptation of motion-sensitive neurons[20]. Given our findings, we predicted that adapting to a large high-contrast moving stimulus should result in a weaker MAE, whereas adaptation to a low-contrast stimulus should not. We explored these predictions by inducing MAE with moving Gabor patches of various sizes and contrasts, and testing MAE strength with a small test stimulus. As predicted, MAE strength decreased with increasing size when observers adapted to a high-contrast Gabor patch, indicating spatial suppression (Fig. 4). This result is consistent with earlier observations[21,22] that were restricted to high-contrast adapting stimuli. In contrast, as predicted, when a low-contrast adapting stimulus was used, MAE strength increased with increasing size.

The present study reveals that large-sized objects detrimentally affect human motion perception, which contradicts intuition and challenges accepted ideas about the spatial properties of motion perception. In psychophysics, spatial summation has often been assumed as a basic characteristic of motion processing[12,13], but we show here that this holds only for conditions of low visibility. In addition, our results corroborate and help to explain some earlier findings. Dividing a large high-contrast object into smaller parts actually improved performance in a speed discrimination task[23], leading to the suggestion of surround suppression as one possible explanation. Increasing the contrast of a briefly presented, large drifting grating decreased performance[24], agreeing with a portion of our findings (filled diamonds in Fig. 1b). Brief motion stimuli, by virtue of their broad temporal frequency spectrum, might therefore stimulate motion filters tuned to opposing directions of motion[24]. At high contrast, these paired filters could saturate impairing direction identification; however, this fails to explain the effects of size that are central to the present study. Moreover, paired opponent filters cannot explain the MAE results (Fig. 4) that generalize our principal findings to prolonged motion stimuli.

For several reasons we believe that our results might reflect the receptive field properties of centre–surround neurons in MT. First, impaired visual performance with larger stimuli has been construed as the perceptual signature expected from antagonistic centre–surround mechanisms[11]. Second, the 'critical size' at which we begin to observe strong surround suppression (Fig. 1b) is large enough to impinge on the surrounds of MT neurons with foveal receptive fields (Fig. 1d). However, this critical size is much larger than receptive fields in the primary visual area (V1) and much smaller than receptive fields in the lateral part of area MST (medial superior temporal), which are cortical areas other than MT that contain centre–surround motion neurons[4,5]. Third, the detrimental effect of stimulus size diminishes in the visual periphery, which is consistent with the increase in sizes of MT receptive fields with eccentricity[6,17]. Fourth, MAE, a perceptual after-effect attributed, at least in part, to MT activity[20], is weaker if induced with large high-contrast stimuli. This result is expected if such stimuli inhibit the activity of MT neurons whose adaptation normally contributes to the MAE. Last, MT neurons respond more weakly to motion of isoluminant gratings than to motion of luminance gratings[25], a property that dovetails nicely with the failure of isoluminant motion to produce surround suppression.

Our conclusion rests on several assumptions, which are not unreasonable given existing evidence. We assume that the quality of motion perception covaries with underlying neuronal firing rate—a reasonable assumption for MT neurons[26]. We also assume that the strength of surround suppression induced by a large moving object is not substantially altered because of the variations in receptive field size and eccentricity. Of course, surrounds of some neurons will be only partly stimulated, particularly those with receptive field centres aligned along the stimulus border. However, because the border of our stimuli is blurred and low in contrast (Fig. 1d), these 'border neurons', too, will be affected by surround

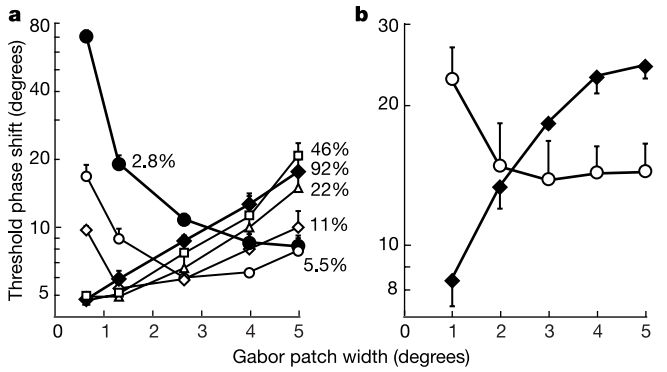

Figure 3 Results from phase-shift and isoluminant-motion experiments. **a**, Phase-shift thresholds as a function of stimulus size at different contrasts. **b**, Phase-shift thresholds as a function of stimulus size for luminance contrast (filled circles) and isoluminant (open circles) stimuli. Results are means ± s.e.m.

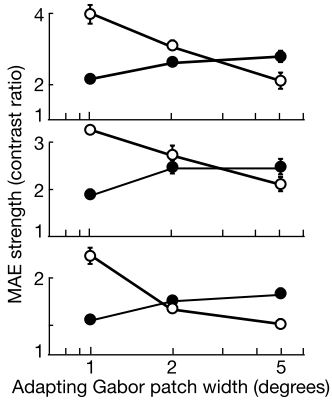

Figure 4 Effects of stimulus size and contrast on the MAE strength for three subjects, A.P. (top), R.B. (middle) and D.T. (bottom). Filled symbols show MAE strength for low-contrast adaptation (2.8%). Empty symbols show results for high-contrast adaptation (26%). Results are means ± s.e.m.

suppression, because their partly stimulated surrounds will receive higher contrast stimulation than their centres. Last, we assume that our results arise from centre–surround neurons, and not the so-called 'wide-field' MT neurons, which show no surround suppression[3]. Centre–surround and wide-field neurons are anatomically segregated[3,6] and produce different behavioural effects when artificially stimulated, leading to the conclusion that wide-field neurons might not be directly involved in signalling object motion[7].

Our results generate testable predictions. First, they predict that response strength in MT to isoluminant motion stimuli, although weak, should increase with stimulus size. Second, the observed contrast dependence of the spatial integration of motion signals is particularly interesting. It predicts contrast-dependent changes in receptive field properties of MT neurons similar to those observed in V1 (refs 14–16), which should be measurable with neurophysiological and neuroimaging techniques.

Why, though, is the nature of centre–surround interactions in motion perception so markedly affected by contrast? At high contrast, the computational benefits of surround suppression[7–10] probably outweigh the obligatory decrease in neuronal activity and reduced sensitivity. At low contrast, high sensitivity is essential, so it makes functional sense that receptive field organization shifts from surround suppression to spatial summation. The integration of motion signals over space is therefore an adaptive process that enables the visual system to process moving stimuli more efficiently by employing computationally important suppressive mechanisms only when the sensory input is strong enough to guarantee visibility. □

Methods

Displays and viewing conditions

Patterns were shown on a monitor with linear display characteristics (800 pixels × 600 pixels resolution, 120 Hz). The main results were confirmed at 160 and 200 Hz. Viewing was binocular at 83 cm. The ambient illumination was 4.8 cd m^{-2}. The background luminance was 60.5 cd m^{-2}. The size was defined as the 2σ width of a Gabor patch, a drifting vertical sine grating windowed by a stationary two-dimensional gaussian envelope (Fig. 1d), where σ is the standard deviation of the gaussian. Duration was defined as 2σ of the temporal gaussian envelope. On each trial, a drifting Gabor patch was presented foveally and observers indicated the perceived direction (left or right) by a key press. Feedback was provided. Duration thresholds (82%) were estimated by interleaved Quest staircases. For each condition, five observers ran four pairs of interleaved staircases; the first pair was discarded as practice. All experiments complied with institutionally reviewed procedures for human subjects.

Visual noise experiment

Speed was increased to 4° s^{-1}. A 20° by 20° noise pattern consisted of 480 × 480 dark and light pixels and was randomly regenerated at 120 Hz. Noise contrast was defined as the luminance difference between light and dark pixels divided by the sum of their luminances. This noise mask was combined additively with a foveally presented Gabor patch (46% contrast). Other methods were the same as in the first experiment.

Eccentric presentation experiment

To present visually larger stimuli within the limited monitor area, a gaussian spatial envelope was replaced with the two-dimensional raised cosine envelope. Size was defined as the distance between two diametrically opposing points on the raised cosine envelope where the contrast was 60.7% of the peak contrast (analogous to the 2σ of a gaussian distribution). Spatial frequency was lowered to 0.5 cycle per degree and the speed was increased to 4° s^{-1}. In this experiment only, motion directions were vertical (up or down). Other methods were the same as in the first experiment.

Isoluminant motion experiment

The Gabor patch consisted of spatially overlapping isoluminant red and green gratings. For each observer, the red–green isoluminant point was obtained with the minimum-motion technique[27]. If isoluminant red and green gratings are presented spatially in antiphase, the resulting red–green compound grating has no luminance contrast. Presenting the same two gratings in phase produces a yellow–black luminance grating. The spatial frequency was 1 cycle per degree. Results similar to those in Fig. 3b were obtained by measuring duration thresholds.

MAE experiment

Observers ($n = 3$) adapted to a foveally centred Gabor patch (1 cycle per degree) moving at 4° s^{-1}. The test stimulus consisted of two overlapping Gabor patches drifting in opposite directions (the stimulus parameters were the same as in the adapting Gabor patch except the width, which was fixed to 1°). When the contrasts of two Gabor patches were identical, the motion was ambiguous and the test stimulus seemed to flicker. Adapting to a motion in one direction effectively decreases the motion strength of the Gabor patch moving in the adapted direction and the test stimulus appears to move in the opposite direction. Then, to restore the perception of flicker, the contrast of the Gabor patch moving in the adapted direction is increased and the contrast of the other Gabor patch is decreased. The contrast ratio required to restore flicker perception is taken as a measure of MAE strength (higher contrast ratio corresponds to stronger MAE). The initial adaptation was for 30 s (10 s 'top-off' adaptation after the first trial), followed by a 0.3-s blank screen and a 1-s test stimulus. After viewing the test stimulus, observers indicated the perceived direction. The contrast ratio of two Gabor patches composing the test stimulus was then adjusted under the control of two interleaved 'one-up—one-down' staircases. Each staircase converged after six reversals, with the average of the last four reversals taken as the result. Eight measurements were made for each condition.

Received 15 January; accepted 9 May 2003; doi:10.1038/nature01800.

1. Allman, J., Miezin, F. & McGuinness, E. Stimulus specific responses from beyond the classical receptive field: Neurophysiological mechanisms for local–global comparisons in visual neurons. *Annu. Rev. Neurosci.* **8,** 407–430 (1985).
2. Allman, J., Miezin, F. & McGuinness, E. Direction- and velocity-specific responses from beyond the classical receptive field in the middle temporal visual area (MT). *Perception* **14,** 105–126 (1985).
3. Born, R. T. & Tootell, R. B. Segregation of global and local motion processing in primate middle temporal visual area. *Nature* **357,** 497–499 (1992).
4. Eifuku, S. & Wurtz, R. H. Response to motion in extrastriate area MSTl: Center–surround interactions. *J. Neurophysiol.* **80,** 282–296 (1998).
5. Jones, H. E., Grieve, K. L., Wang, W. & Sillito, A. M. Surround suppression in primate V1. *J. Neurophysiol.* **86,** 2011–2028 (2001).
6. Raiguel, S. E., van Hulle, M. M., Xiao, D. K., Marcar, V. L. & Orban, G. A. Shape and spatial distribution of receptive fields and antagonistic motion surround in the middle temporal area (V5) of the macaque. *Eur. J. Neurosci.* **7,** 2064–2082 (1995).
7. Born, R. T., Groh, J. M., Zhao, R. & Lukasewycz, S. J. Segregation of object and background motion in visual area MT: Effects of microstimulation on eye movements. *Neuron* **26,** 725–734 (2000).
8. Nakayama, K. & Loomis, J. M. Optical velocity patterns, velocity-sensitive neurons, and space perception: A hypothesis. *Perception* **3,** 63–80 (1974).
9. Gautama, T. & Van Hulle, M. M. Function of center–surround antagonism for motion in visual area MT/V5: A modeling study. *Vision Res.* **41,** 3917–3930 (2001).
10. Buracas, G. T. & Albright, T. D. Contribution of area MT to perception of three-dimensional shape: Computational study. *Vision Res.* **361,** 869–887 (1996).
11. Westheimer, G. Spatial interaction in human cone vision. *J. Physiol. (Lond.)* **190,** 139–154 (1967).
12. Anderson, S. J. & Burr, D. C. Spatial summation properties of directionally sensitive mechanisms in human vision. *J. Opt. Soc. Am. A* **8,** 1330–1339 (1991).
13. Watson, A. B. & Turano, K. The optimal motion stimulus. *Vision Res.* **35,** 325–336 (1995).
14. Kapadia, M. K., Westheimer, G. & Gilbert, C. D. Dynamics of spatial summation in primary visual cortex of alert monkeys. *Proc. Natl Acad. Sci. USA* **96,** 12073–12078 (1999).
15. Levitt, J. B. & Lund, J. S. Contrast dependence of contextual effects in primate visual cortex. *Nature* **387,** 73–76 (1997).
16. Sceniak, M. P., Ringach, D. L., Hawken, M. J. & Shapley, R. Contrast's effect on spatial summation by macaque V1 neurons. *Nature Neurosci.* **2,** 733–739 (1999).
17. Albright, T. D. Direction and orientation selectivity of neurons in visual area MT of the macaque. *J. Neurophysiol.* **52,** 1106–1130 (1984).
18. Nakayama, K. & Silverman, G. H. Detection and discrimination of sinusoidal grating displacements. *J. Opt. Soc. Am. A* **2,** 267–274 (1985).
19. Dobkins, K. R. & Albright, T. D. in *High-level Motion Processing* (ed. Watanabe, T.) 53–94 (MIT Press, Cambridge, Massachusetts, 1998).
20. Huk, A. C., Ress, D. & Heeger, D. J. Neuronal basis of the motion aftereffect reconsidered. *Neuron* **32,** 161–172 (2001).
21. Murakami, I. & Shimojo, S. Modulation of motion aftereffect by surround motion and its dependence on stimulus size and eccentricity. *Vision Res.* **35,** 1835–1844 (1995).
22. Sachtler, W. L. & Zaidi, Q. Effect of spatial configuration on motion aftereffects. *J. Opt. Soc. Am. A* **10,** 1433–1449 (1993).
23. Verghese, P. & Stone, L. S. Perceived visual speed constrained by image segmentation. *Nature* **381,** 161–163 (1996).
24. Derrington, A. M. & Goddard, P. A. Failure of motion discrimination at high contrasts: Evidence for saturation. *Vision Res.* **29,** 1767–1776 (1989).
25. Gegenfurtner, K. R. *et al.* Chromatic properties of neurons in macaque MT. *Vis. Neurosci.* **11,** 455–466 (1994).
26. Britten, K. H., Shadlen, M. N., Newsome, W. T. & Movshon, J. A. The analysis of visual motion: A comparison of neuronal and psychophysical performance. *J. Neurosci.* **12,** 4745–4765 (1992).
27. Cavanagh, P., MacLeod, D. I. & Anstis, S. M. Equiluminance: Spatial and temporal factors and the contribution of blue-sensitive cones. *J. Opt. Soc. Am. A* **4,** 1428–1438 (1987).
28. Sclar, G., Maunsell, J. H. & Lennie, P. Coding of image contrast in central visual pathways of the macaque monkey. *Vision Res.* **30,** 1–10 (1990).
29. Rees, G., Friston, K. & Koch, C. A direct quantitative relationship between the functional properties of human and macaque V5. *Nature Neurosci.* **3,** 716–723 (2000).
30. Kastner, S. *et al.* Modulation of sensory suppression: Implications for receptive field sizes in the human visual cortex. *J. Neurophysiol.* **86,** 1398–1411 (2001).

Acknowledgements We thank J. Schall, B. Borghuis, S. Shorter-Jacobi and A. Panduranga for comments on the experiments and manuscript. This work was supported by a grant from the NIH.

Competing interests statement The authors declare that they have no competing financial interests.

Correspondence and requests for materials should be addressed to D.T. (duje.tadin@vanderbilt.edu).